Asian Journal of Urology (2017) 4, 201–207

Available online at www.sciencedirect.com

ScienceDirect

journal homepage: www.elsevier.com/locate/ajur

Asian Focus

Effect of *Blumea balsamifera* extract on the phase and morphology of calcium oxalate crystals

Charlimagne M. Montealegre*, Rizalinda L. De Leon

Department of Chemical Engineering, College of Engineering, University of the Philippines Diliman, Quezon City, Philippines

Received 28 January 2016; received in revised form 23 March 2016; accepted 1 June 2016
Available online 3 September 2016

KEYWORDS
Kidney stones;
Calcium oxalate stone;
Blumea balsamifera extract;
Microscopy;
Calcium oxalate dihydrate

Abstract *Objective:* Calcium oxalate crystals are found in majority of kidney stones with calcium oxalate monohydrate (COM) as one of the primary types of kidney stones. Various methods of treatment exist, including herbal treatment in the Philippines that uses the medicinal herb *Blumea balsamifera* (*B. balsamifera*).
Methods: The effect of *B. balsamifera* extract on the morphology of calcium oxalate crystals was studied by light microscopy, image analysis, powder X-ray diffraction and scanning electron microscopy.
Results: The extract decreased the crystal size by 5.22%–82.62% depending on the degree of supersaturation. Through analysis of the projected area of the crystals, the extract was found to shift the phase of the crystals from COM to calcium oxalate dihydrate (COD). This shift in phase is significant with a COM to COD shift of 88.26% at 0.5 mg/mL of extract and 91.53% at 1.0 mg/mL of extract. Scanning election microscopic (SEM) images revealed aggregation of crystals at 0 mg/mL of extract. At 1.0 mg/mL of extract, the scanning electron micrographs showed discernible crystal unit boundaries.
Conclusion: B. balsamifera extract was observed to have decreased crystal size, shifted crystal phase from COM to COD and prevented the aggregation of calcium oxalate crystals.

* Corresponding author.
E-mail address: charlimagne.montealegre@coe.upd.edu.ph (C.M. Montealegre).
Peer review under responsibility of Second Military Medical University.

http://dx.doi.org/10.1016/j.ajur.2016.08.009

1. Introduction

Kidney stones have always been a prevalent health problem facing mankind. Kidney stones are made up of biomolecules such as antibodies and proteins, minerals such as calcium oxalate monohydrate (COM, $CaC_2O_4 \cdot H_2O$), calcium oxalate dihydrate (COD, $CaC_2O_4 \cdot 2H_2O$), calcium phosphate, struvite ($MgNH_4PO_4 \cdot 6H_2O$) and uric acid [1—3]. Some kidney stones are made of cysteine, but the most pathologically prevalent are COM stones. An analysis of kidney stone cases found COM in 99% of extracted stones [1], and in 68% of the cases, COM was identified as the main stone component [4]. The hydrates of calcium oxalate have been found to exhibit distinct crystalline structures depending on their degree of hydration. The monohydrate phase (COM) has a crystalline structure of elongated rhombohedron units. It has a distinct hexagonal projection along its 010 face [5—7]. Various studies showed that the dihydrate phase (COD) has an octahedral or square-bipyramid structure with a distinct square projection [5,8,9].

The growth of COM crystals is influenced by the presence of growth modifiers that have a wide nature from inorganic compounds, to biologically-produced and synthetic organic compounds. Some studies explored the growth modifying properties of herbal treatment to urinary calculi. The extract of Khella plant was found to influence the crystallization process. In the presence of the extract, more COD than COM crystals are formed relative to the control [5]. A mallorcan herbal preparation containing extracts and tinctures of *Zea mays*, bearberry, *Sabal serrulata* and others, reduced the calcium deposition in renal tissue of ethylene glycol gavaged rats [10]. Polysaccharide-based biopolymers such as gum arabic were also shown to stabilize the formation of COD with a tetragonal bipyramid or octahedral morphology [11].

Bergenia ciliata rhizome extract was found to decrease the absorbance of crystallizing solutions with artificial urine. Based on this decrease in absorbance with the control solution, a dose dependent inhibition of 58%—97% was reported [12]. COM and COD crystals were also found to decrease, however this was solely based on the qualitative appraisal of the crystal micrographs and lacked quantification. These effects were attributed to the polyphenolics in the extract such as saponins, alkaloids, flavonoids and terpenoids. Studies involving the crystal growth inhibition of plant extracts are limited, yet treatment had been in existence for thousands of years and was even mentioned in ancient Egyptian texts [13].

A decoction of the leaves of *Blumea balsamifera* (*B. balsamifera*) is reported to have anti-lithogenic effects and is a means of treating kidney stones. This therapeutic effect was attributed to the diuretic effect of *B. balsamifera* [14], but based on the study of Rodgers et al. [15] it could not be concluded that the therapeutic effect is merely based on this property. More so, *B. balsamifera* contains several compounds which could have an inhibitory effect on COM stone formation.

How *B. balsamifera* influences the crystallization process of calcium oxalate has not been fully explored. This study aims to fill part of that knowledge gap by investigating the effect of *B. balsamifera* extract on the phase and morphology of calcium oxalate crystals formed from supersaturated calcium ion and oxalate ion solutions.

2. Materials and methods

The effect of *B. balsamifera* extract on the morphology of calcium oxalate crystals was investigated through light microscopy, image analysis, powder X-ray diffraction and scanning electron microscopy. All solutions used throughout the experiment were prepared with deionized water.

2.1. Extract preparation

The extract of *B. balsamifera* was prepared from a decoction of commercially available Golden Spoon™ (Seamaxx Enterprises, Manila, Philippines) organic plants all natural sambong tea. The Golden Spoon™ claims to be made of pure handpicked *B. balsamifera* leaves. The leaves were boiled in deionized water for 5 min. The liquid part was filtered with a cellulose filter paper and transferred to a volumetric flask. Repeated washings of boiling deionized water was used until a clear liquid was achieved. The decoction was cooled prior to final adjustment of the volume. A fresh decoction with a concentration of 5 mg dried leaves per mL solution was prepared prior to its application. Different concentrations of the extract were prepared from the freshly prepared decoction. The required amount of extract was mixed with crystallization solutions and diluted with deionized water to final volume.

2.2. Light microscopy

Crystals were grown by reactive precipitation of calcium chloride and sodium oxalate solutions in single-use polypropylene cuvettes. These are stored for 72 h at room temperature to reach equilibrium. The contents of the cuvette were then stirred, a sample was gathered and mounted in a hemocytometer and observed under a light microscope. Micrographs were taken and the images were subject to image analysis by ImageJ v1.47t (https://imagej.nih.gov/ij/download.html) to measure the crystal size. Shape was quantified by using the ratio between the maximum Feret diameter and minimum Feret diameter.

2.3. Powder X-ray diffraction and scanning electron microscopy

Crystals were prepared by bulk crystallization. Required amounts of water, extract, sodium oxalate solution, and calcium chloride solution were then mixed. The solution was covered with a film and left undisturbed for 3 days. Crystals were harvested by centrifugation at 2504 $\times$ *g* for 30 min. The supernatant was discarded and the crystals were dried in a desiccator for 3 days. The dried crystals were sealed and maintained in the desiccator prior to analyses.

Samples were analyzed by powder X-ray diffraction using Rigaku Miniflex II and Hitachi S3400N Scanning Electron Microscope (SEM) (The analysis was performed at the Department of Chemical Engineering, University of the Philippines Diliman, Quezon City, Philippines). Magnification and electron beam voltage were adjusted accordingly.

2.4. Design of experiment

The effect of the extract on the morphology and nucleation of the crystal was studied at various degrees of supersaturation and extract levels. The degree of supersaturation was varied from 10.0, 12.5, 15.0, 17.5, to 20.0. These degrees of supersaturation are based on the solubility of COM at 25°C calculated as:

$$S = \sqrt{\frac{[Ca^{2+}]\left[C_2O_4^{2-}\right]}{K_{sp,\ 25°C}}}$$

The concentration of calcium and oxalate was maintained at a 1:1 ratio since studies showed that changes in their proportion also influence the morphology of the crystals produced. Literature data for the solubility product constant will be adopted, i.e., $K_{sp,25°C} = 10^{-8.69}$ [16]. Thus at a supersaturation of 10, the molarity of calcium chloride and sodium oxalate are equivalent to a value of 0.4519 mmol/L.

The level of extract addition was limited to 3: the blank 0 mg/mL, 0.5 mg/mL and 1.0 mg/mL. This means of expressing the concentration refers to the ratio of mass of dried leaves used in the preparation of the decoction to the final volume of the solution formed after the extract was added to the crystallization solution.

3. Results and discussion

COM is primarily, if not solely formed across all degrees of supersaturation whenever the extract is absent from the crystallization solution as shown in Fig. 1. The COM crystals are easily identified by their characteristic hexagonal shape. In solutions without the extract, the crystals are also limited in number but greater in size. Heterogeneous growth is also observed at higher supersaturations. Figs. 2 and 3 show that in the presence of extract in the solution, the size of crystals formed after 72 h is significantly smaller than those formed in the absence of extract, while the amount of crystals in the micrograph increases as the size decreases. The square projection of the octahedral COD crystals dominates these micrographs.

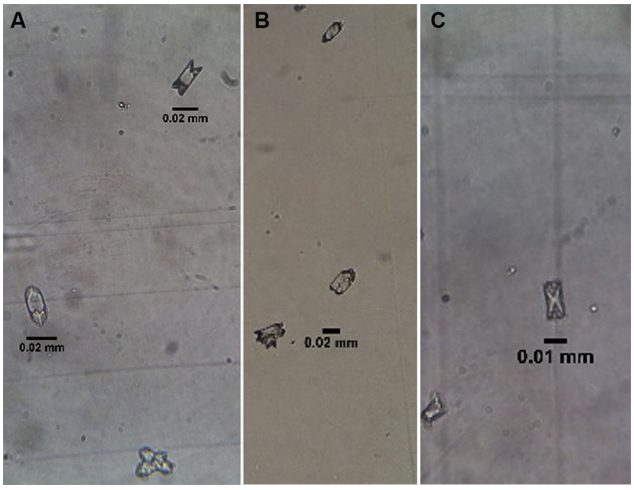

Figure 1 Micrograph at a supersaturation of 10.0 (A), 15.0 (B) and 20.0 (C) with 0 mg/mL of extract. A small number of calcium oxalate monohydrate crystals are observed across all degrees of supersaturation (A and C are at × 640 while B is at × 160).

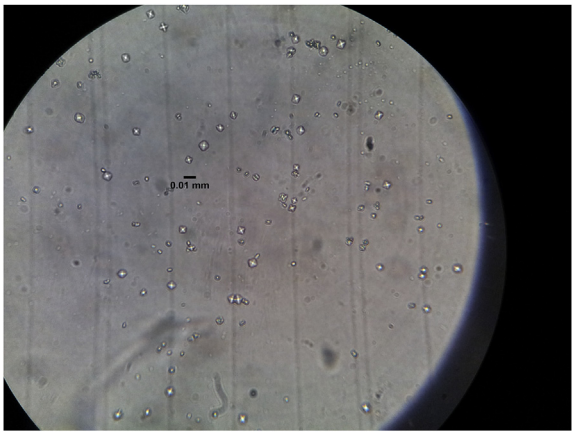

Figure 2 The micrograph at a supersaturation of 20.0 with 0.5 mg/mL of extract shows crystal formation dominated by calcium oxalate dihydrate crystals (×640).

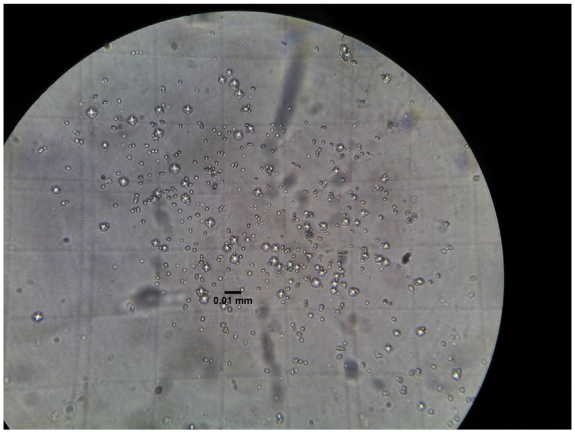

Figure 3 The micrograph at a supersaturation of 20.0 with 1.0 mg/mL of extract shows increased crystal formation dominated by calcium oxalate dihydrate crystals (×640).

The micrographs were then subjected to image analysis using the software ImageJ. Treatments such as adjustment of brightness, contrast and conversion to the required formatting were done on the micrographs until these were suitable for image analysis and the particles could be characterized in terms of their size and shape.

3.1. Crystal size

The size of the particles is reported as the Feret diameter (d_F) and equivalent circle diameter (d_{eq}). The particle size distribution (PSD) of the crystals based on d_F and d_{eq} are determined. Figs. 4 and 5 show the particle size distribution for a supersaturation level of 20 containing 0 mg/mL of extract. As it is defined, d_F is inherently greater than d_{eq} or equal when the particle measured is a circle. The crystals

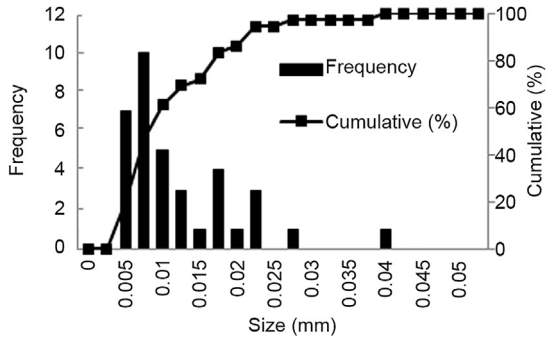

Figure 4 Feret diameter particle size distribution for a supersaturation 20 without extract. The mode and median occurred at 0.0075 mm (two-sample paired t-test, $p < 0.075$).

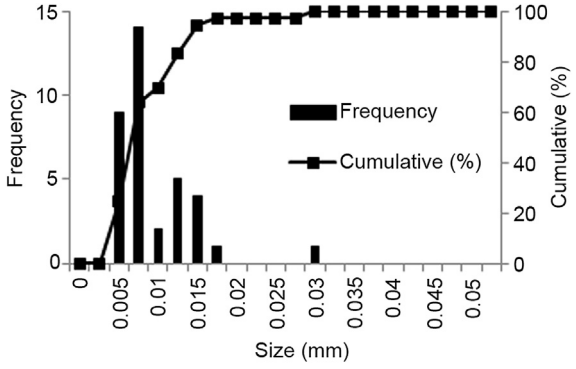

Figure 5 Equivalent circle diameter particle size distribution for a supersaturation 20 without extract. The mode and median occurred at 0.0075 mm similar to the Feret diameter particle size distribution (two-sample paired t-test, $p < 0.075$).

of COM and COD have diagonals that are longer than the equivalent circle diameter. The PSD for d_F also covers a wider range compared to that for the d_{eq}.

Presenting the particle diameter as d_F or d_{eq} as an arithmetic or area mean would result into four possible ways of presenting the particle size. The arithmetic mean and area mean of the d_F and d_{eq} are summarized in Fig. 6.

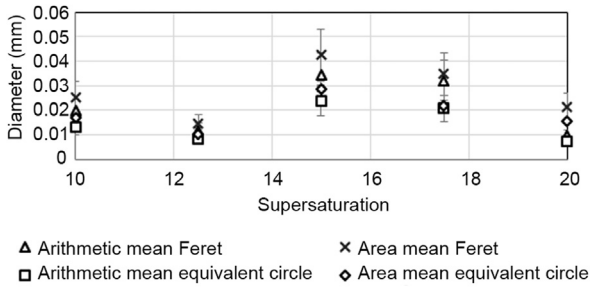

Figure 6 Mean diameters for various degrees of supersaturation containing 0 mg/mL of extract. Regardless of the method of expressing the diameter, it generally decreases with increasing supersaturation with a discontinuity between a supersaturation of 12.5 and 15.0.

The area mean diameters are consistently greater than the arithmetic means due to the equal contribution of the large and small particles to the mean diameter. Fig. 6 also shows that the highest diameters were reported for area mean d_F, followed by arithmetic mean d_F, area mean d_{eq} and the least is for arithmetic mean d_{eq}. The relative standard deviation across supersaturation levels are 23.24%—26.93% except for the supersaturation of 20 where the relative standard deviation reached up to 46.54%. Regardless of the method for presenting the mean, the diameters and their combinations, the trends in the change of the diameter with respect to the degree of saturation are similar. Increasing the supersaturation decreases the diameter of the crystal. This is true from a supersaturation degree of 10—12.5 and 15—20 but a jump discontinuity is observed between 12.5 and 15.

Upon the addition of *B. balsamifera* extract, the size of the crystals are essentially constant across all degrees of supersaturation and extract concentration with an area mean d_F of (9.63 $\pm$ 0.76) μm corresponding to a relative standard deviation of 7.84%.

The mean diameters changed dramatically ranging from 5.22% to 82.69% (depending on the type of mean and diameter) with respect to the untreated systems as shown in Fig. 7. The reduction in crystal size is highest at a supersaturation of 15.0 and on average, smallest at a supersaturation of 12.5.

3.2. Crystal shape

The shape of the crystal is indicative of its type. Fig. 8 shows the typical projections observed from the micrographs of the crystals. COM crystals are composed of elongated rhombohedron units exhibiting a hexagonal projection along its (010) and $(10\bar{1})$ faces shown in Fig. 8A and B respectively. COD crystals are octahedral with a square or diamond shaped projection shown in Fig. 8C. These distinct crystal morphologies are used as the primary means of differentiating between the calcium oxalate hydrates. Fig. 8D shows a short dumbbell-shaped projection of a calcium oxalate trihydrate crystal. This morphology was only observed once in this study.

Aspect ratio is used to differentiate between COM and COD crystals. Crystals with an aspect ratio greater than 1.5 are classified as COM. To determine the relative abundance

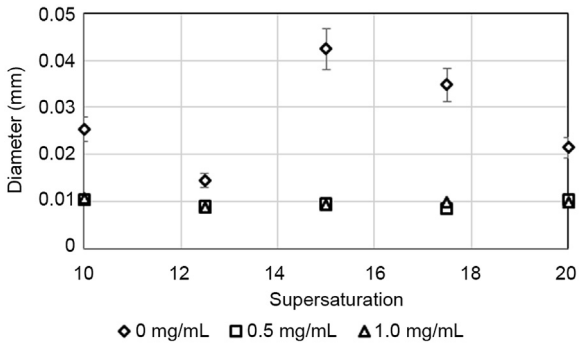

Figure 7 Crystal size decreased drastically at 0.5 and 1.0 mg/mL of extract across all levels of supersaturation.

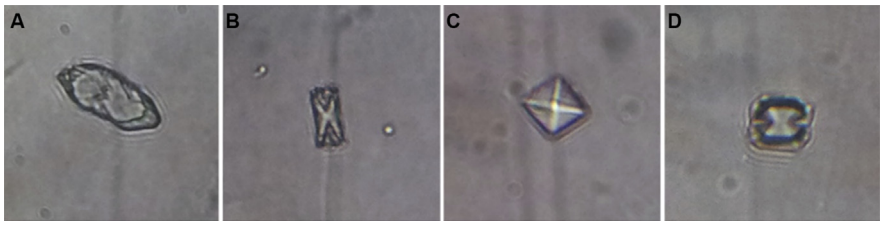

Figure 8 Micrographs of calcium oxalate crystals. (A) The (010) face of a calcium oxalate monohydrate crystal. (B) $10\bar{1}$ face of calcium oxalate monohydrate crystal. (C) Top view of the octahedral calcium oxalate dihydrate crystal. (D) Dumbell shaped cross section characteristic of a calcium oxalate trihydrate crystal.

of COM and COD crystals formed, the projected area of crystals identified as COM is summed and its fraction to the total projected area is calculated. Fig. 9 summarizes the COM fractions at varying degrees of supersaturation and extract levels.

Fig. 9 shows that COM crystals are predominantly present at 0 mg/mL of extract. The presence of the extract at 0.5 mg/mL and 1.0 mg/mL dramatically shifted the morphology of the crystals into the formation of COD. The area fraction of COM crystals changed from an average of 0.9932 ± 0.0122 without the extract to 0.1158 ± 0.1287 and 0.0842 ± 0.0928 at 0.5 and 1.0 mg/mL of extract respectively. This corresponds to an average COM area fraction reduction of (88.26 ± 13.03) at 0.5 mg/mL and (91.53 ± 9.29) at 1.0 mg/mL. The high standard deviation of the percent reduction implies that there is no significant difference between an extract level of 0.5 or 1.0 mg/mL. Various studies on growth modifiers reported a similar COM to COD shift [5,7,16] but only in this study is this shift quantified.

Some microscopy observations that are difficult to quantify by the methods mentioned above, were not included in the analysis. An example of such observation is shown in Fig. 10. This was observed at a supersaturation of 17.5.

This could be explained by a high degree of heterogeneous nucleation that is out of the scope of this study. The cross-shaped structure may be a result of over growth in the $01\bar{1}$ and 011 faces of COM. These were only observed at supersaturation levels of 17.5 and 20 in the absence of the extract. At these conditions it is possible that the crystal

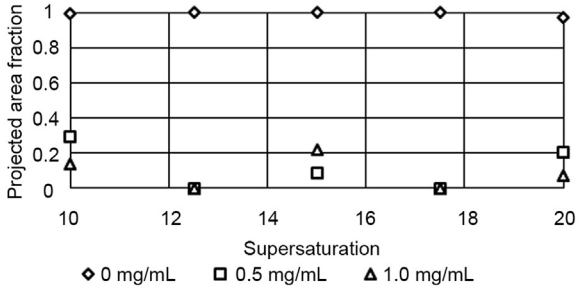

Figure 9 Calcium oxalate monohydrate dominated the projected are fraction at 0 mg/mL of extract. Presence of the extract resulted into a decrease of calcium oxalate monohydrate fraction suggesting a dominant formation of calcium oxalate dihydrate crystals.

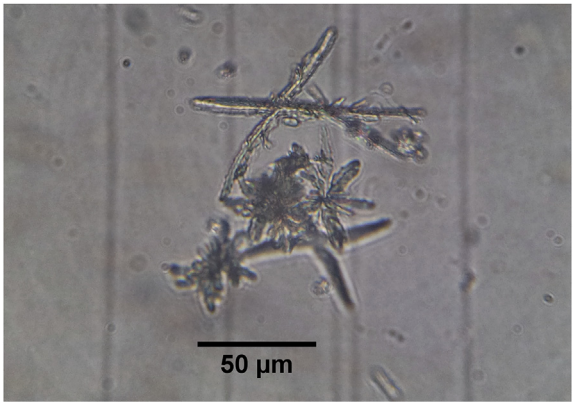

Figure 10 A structure forming from aggregated crystals with a high degree of branching and inter-crystal growth.

habit is altered. The fact that highly aggregated structures like those shown in Fig. 10 are only observed when the extract is absent from the crystallization solution suggests an inhibiting action of the extract towards aggregation and the observed overgrowth.

3.3. Powder X-ray diffraction and scanning electron microscopy

The crystals produced from a supersaturation of 20 were air dried. The powder X-ray diffraction spectra show strong peaks, indicating the crystalline nature of the samples.

Fig. 11 shows that at 0.1 mg/mL of extract, the characteristic peaks for COM [17] have the highest intensities. However, at 1.0 mg/mL of extract the intensities of the peaks for COM are very low relative to stronger peaks at 2θ positions 44.5°, 64.8° and 77.86° indicating the (200) and (211) faces of a tetragonal crystal [18]. The intensity of the spectra supports the observation that at low extract concentrations COM crystals are predominantly formed and at the highest extract concentration of 1.0 mg/mL, the peaks for COM are observed but at a relatively very low intensity compared with peaks related to the (200) face of a tetragonal crystal which may indicate COD. A comparison with the micrographs in Fig. 3 suggests that these strong peaks may be attributed to COD.

Micrographs were taken using a SEM, shown in Fig. 12.

Fig. 12C shows how the crystal morphology changed at the highest degree of supersaturation 20. In Fig. 12A without the extract, it is difficult to discern the boundaries

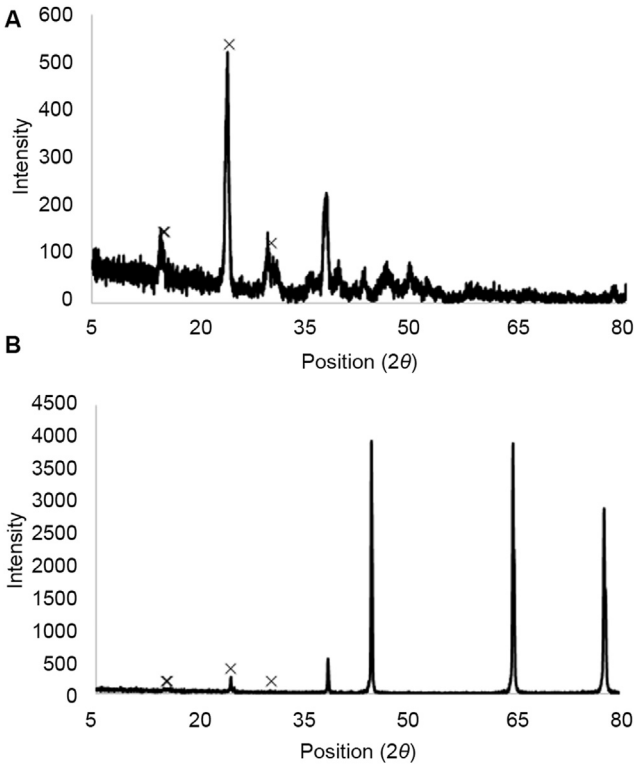

Figure 11 The powder X-ray diffraction spectra of samples at a supersaturation of 20.0 and an extract level of 0.1 mg/mL (A), and at 1.0 mg/mL (B) show strong peaks. Crossmarks refer to characteristic peaks for calcium oxalate monohydrate [17].

between crystals suggesting heterogeneous growth resulting to merging of different crystal units. In Fig. 12B, a slight addition of the extract at 0.1 mg/mL resulted into individual crystal units that are discernible. Aggregation is observed but a lot less than the former. Crystals in Fig. 12C were grown at an extract concentration of 1.0 mg/mL. The crystal units are separate, smaller and the shape is discernible. Crystal shapes characteristic of the (010) and (101) side of COM is evident. Majority of the crystal formed also had a low aspect ratio evident from its square projection. These observations evidently support an earlier claim made, i.e., *B. balsamifera* extract minimizes crystal aggregation aside from modifying the morphology.

The results showed that *B. balsamifera* extract decreased the crystal size, shifted the phase of the crystals into COD and inhibited crystal aggregation. This may be the effect of modification in the solution properties of the crystallization medium brought about by the addition of compounds, in this case phytochemicals in the *B. balsamifera* extract. Such effects have been observed even at very low concentrations [7]. A similar change in solution property due to a plant extract was reported as the surface free energy decreased due to Khella plant extract [5].

4. Conclusion

Micrographs taken at different levels of supersaturation and extract concentration exhibited a marked difference in terms of crystal size and shape. Analysis of the crystal size in terms of the mean Feret and equivalent circle diameters showed that at 0.5 and 1.0 mg/mL of extract, the size decreased by 5.22%—82.69%, depending on the degree of saturation. Crystals were classified as COM or COD depending on the aspect ratio. It was found that the extract reduced the projected area fraction of COM crystals from an average of 0.9932 $\pm$ 0.0122 to 0.1158 $\pm$ 0.1287 at 0.5 mg/mL of extract and 0.0842 $\pm$ 0.0928 1.0 mg/mL of extract suggesting a shift of crystal phase from COM to COD.

The extract decreased the crystal size, shifted the phase of the crystals into COD and inhibited crystal aggregation. This could be beneficial in the prevention of stone formation. Not only will the formed crystals be smaller, but the implication that these crystals might have a lower likelihood of aggregation shows that the crystals formed could more easily be eliminated by natural means. This is very beneficial for stone formers since studies suggest that the biochemical pathways of a stone former will always promote stone formation but the presence of growth modifiers such as phytochemicals found in *B. balsamifera* could aid in the elimination of stone.

Conflicts of interest

The authors received research grants from the Engineering Research and Development for Technology (ERDT) program by the Department of Science of Technology. The authors declare that they have no conflict of interest.

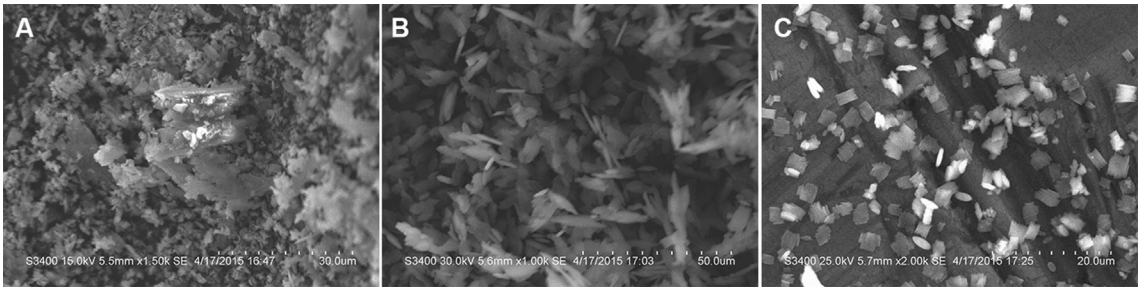

Figure 12 Scanning electron microscope micrograph. (A) for a supersaturation 20.0 without the extract shows indiscernible crystal boundaries. (B) At a supersaturation 20.0 with 0.1 mg/mL of extract discernible crystal boundaries were observed. (C) Distinct crystal boundaries were observed at a supersaturation 20.0 with 1.0 mg/mL of extract.

This article does not contain any studies with human participants or animals performed by any of the authors.

Acknowledgements

The proponents of the study would like to thank the U.P. Engineering Research and Development for Technology (UPERDT) for the financial support and the National Institute for Science and Mathematics Education Development in Philippines for their valuable assistance in the sourcing of some reagents used in this study.

References

[1] Kirejczyk JK, Porowski T, Filonowicz R, Kazberuk A, Stefanowicz M, Wasilewska A, et al. An association between kidney stone composition and urinary metabolic disturbances in children. J Pediatr Urol 2014;10:130—5.
[2] Canales BK, Anderson L, Higgins L, Ensrud-Bowlin K, Roberts KP, Wu B, et al. Proteome of human calcium kidney stones. Urology 2010;76:1017.e13—20.
[3] Siddiqui AA, Mushtaq S. Urolithiasis. London: Springer London; 2012.
[4] Hughes P. The CARI guidelines. Kidney stones epidemiology. Nephrol Carlt 2007;12(Suppl 1):S26—30.
[5] Abdel-Aal EA, Daosukho S, El-Shall H. Effect of supersaturation ratio and Khella extract on nucleation and morphology of kidney stones. J Cryst Growth 2009;311:2673—81.
[6] Farmanesh S, Chung J, Chandra D, Sosa RD, Karande P, Rimer JD. High-throughput platform for design and screening of peptides as inhibitors of calcium oxalate monohydrate crystallization. J Cryst Growth 2013;373:13—9.
[7] Farmanesh S, Ramamoorthy S, Chung J, Asplin JR, Karande P, Rimer JD. Specificity of growth inhibitors and their cooperative effects in calcium oxalate monohydrate crystallization. J Am Chem Soc 2014;136:367—76.
[8] Jung T, Kim WS, Choi CK. Biomineralization of calcium oxalate for controlling crystal structure and morphology. Mater Sci Eng C 2004;24:31—3.
[9] Goiko M, Dierolf J, Gleberzon JS, Liao Y, Grohe B, Goldberg HA, et al. Peptides of Matrix Gla protein inhibit nucleation and growth of hydroxyapatite and calcium oxalate monohydrate crystals. PLoS One 2013;8:e80344.
[10] Grases F, Prieto RM, Gomila I, Sanchis P, Costa-Bauzá A. Phytotherapy and renal stones: the role of antioxidants. A pilot study in Wistar rats. Urol Res 2009;37:35—40.
[11] Gangu KK, Tammineni GR, Dadhich AS, Mukkamala SB. Control of phase and morphology of calcium oxalate crystals by natural polysaccharide. Gum Arab Mol Cryst Liq Cryst 2014;591:114—22.
[12] Saha S, Verma RJ. Inhibition of calcium oxalate crystallisation in vitro by an extract of *Bergenia ciliata*. Arab J Urol 2013;11:187—92.
[13] History of kidney stones — kidney Stoners.org. 2014. http://www.kidneystoners.org/information/history-of-stones/ [accessed 07.11.14].
[14] Alok S, Jain SK, Verma A, Kumar M, Sabharwal M. Pathophysiology of kidney, gallbladder and urinary stones treatment with herbal and allopathic medicine: a review. Asian Pac J Trop Dis 2013;3:496—504.
[15] Rodgers AL, Allie-Hamdulay S, Jackson GE, Durbach I. Theoretical modeling of the urinary supersaturation of calcium salts in healthy individuals and kidney stone patients: precursors, speciation and therapeutic protocols for decreasing its value. J Cryst Growth 2013;382:67—74.
[16] Jung T, Kim WS, Kyun Choi C. Crystal structure and morphology control of calcium oxalate using biopolymeric additives in crystallization. J Cryst Growth 2005;279:154—62.
[17] Akyol E, Öner M. Controlling of morphology and polymorph of calcium oxalate crystals by using polyelectrolytes. J Cryst Growth 2014;401:260—5.
[18] King H, Ferguson S. An X-ray diffraction study of PMN—PT ceramics near the morphotropic phase boundary. Proc Int Conf Sonar Sens Syst 2002;2.